Rytömaa, Samuli; Laine, Sampo; Viitala, Raine

Rotordynamic Investigation of Roll Bouncing Phenomenon in Two-Drum Winder

Published in:
Advances in Mechanism and Machine Science - Proceedings of the 16th IFToMM World Congress 2023—Volume 1

DOI:
10.1007/978-3-031-45705-0_86

Published: 01/01/2023

Document Version
Peer-reviewed accepted author manuscript, also known as Final accepted manuscript or Post-print

Please cite the original version:
Rytömaa, S., Laine, S., & Viitala, R. (2023). Rotordynamic Investigation of Roll Bouncing Phenomenon in Two-Drum Winder. In M. Okada (Ed.), Advances in Mechanism and Machine Science - Proceedings of the 16th IFToMM World Congress 2023—Volume 1 (pp. 885-894). (Mechanisms and Machine Science; Vol. 147). Springer. https://doi.org/10.1007/978-3-031-45705-0_86

Rotordynamic Investigation of Roll Bouncing Phenomenon in Two-Drum Winder

Samuli Rytömaa*, Sampo Laine, and Raine Viitala

Department of Mechanical Engineering, Aalto University, Finland
corresponding author: samuli.rytomaa@aalto.fi
https://www.aalto.fi/en/department-of-mechanical-engineering

Abstract. In paper manufacturing, the vibration caused by roll bouncing is one of the factors limiting the productivity of a two-drum winder. As paper roll rotational speed intersects with natural frequencies of the winder system during the winding cycle, resonance occurs leading to roll bouncing and high vibration levels. To help understand the phenomenon, a simulation model of a two-drum winder is investigated. The model includes the unbalance, changing rotational speed and increasing paper roll diameter. The model is based on finite-element method, including the rotordynamic effects. An example winder geometry is used to demonstrate the simulation capabilities using modal and forced response analysis. The results indicate that the model is capable of capturing the roll bouncing problem and agrees qualitatively with previous research. The model can be used to improve winder designs and therefore increase their productivity.

Keywords: Paper industry · Two-drum winder · rotordynamics · Roll bouncing.

1 Introduction

One of the global megatrends is the increasing demand of paper based products such as tissue and packaging materials [1]. This calls for increased production capacity for paper machines. At the end of paper manufacturing processes, the paper web is wound onto customer rolls using a winder. This is a discontinuous process with acceleration and deceleration between customer roll set changes, which results in higher operating speed requirement when compared to the rest of the paper machine. There are multiple types of winders, of which the most productive one is a two-drum winder. In the two-drum winder, the paper web is wound onto rolls that sit on top of two drums and a third roller is used to keep the paper rolls in place. In case of slitting winder, the jumbo roll is first unwound, then cut into multiple webs and finally rewound into customer rolls on a shared axis [2]. The basic configuration of the rewinding part of a two-drum winder is presented in Figure 1. Roll bouncing is a common problem that is associated with two-drum winders. In short, as more material is wound onto the rolls, increasing vibrations are observed on a frequency equal to the rotational speed of the paper

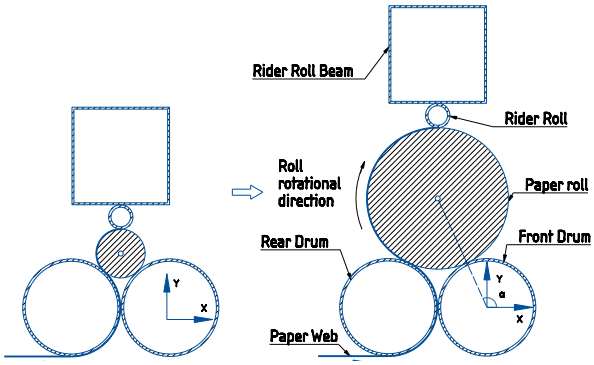

Fig. 1: Main components of a two-drum winder. The paper rolls rest on the two steel drums, and they are kept in place using the rider roll. The rider roll beam supports the rider roll. The winding cycle starts with small roll diameter (left) and ends with large paper roll diameter (right). The angle α represents the angle of contact between the roll and drums. Image is not in scale.

roll. Therefore, it has been proposed that it is caused by roll unbalance [3, 4]. This bouncing can lead to severe lateral vibrations in the winder structure and in worst cases roll throw out. A simple and effective solution is to reduce the web speed, which in turn reduces the rotational speeds and the productivity of the winder. To avoid decreasing the web speed, improved modelling and mitigation methods of the lateral vibrations are required to increase winder productivity to match the increasing speed of the rest of the paper machine.

There are several unique features associated with two-drum winder, which are not present in other large rotating machinery. The most obvious of these is the increasing mass of the paper roll. As more material is wound to the roll, its diameter, and therefore the mass, increases throughout the winding cycle. Increasing diameter leads to the need of decreasing rotational speed constantly to keep the surface speed of the roll constant. The roll surface speed needs to match the constant web speed that is used to feed the winder. The different rolls are in constant contact with each other, coupling their dynamic behavior. The rolling contact between the paper roll and drum is a complex process and influences the final paper roll quality [4]. Finally, the rolls have a developing eccentricity that results in increasing unbalance. All these features are natural to the two-drum winder, and lead to the system being highly non-linear [5].

Previous published research on the modelling of winder dynamics is scarce. Most recent published research is by Jorkama and Von Hertzen [6], the study simplified the problem into a combination of masses and springs. The calculation results were in good agreement with measurements. However, the model presented was unable to differentiate the effect of flexible drums from roll movement on bearings. Simulation of high speed shafted winding machine have been

conducted by [7]. Most of the recent published winding research has focused on how the winding process affects the paper roll internal stresses and final roll quality [8, 9].

This paper presents a simulation model for the two-drum winder that is capable of efficiently handling the unique features associated with the machine, which are the increasing paper roll diameter and the changing rotational speed. It improves on the previous published two-winder simulation by including the flexible rotors, rotor gyroscopic effects and increasing unbalance load. It is shown that the model can capture the roll bouncing phenomenon and provide more detail when compared to previous research. The model can be used to gain insight on the winder dynamics, and how different parameters affect the performance and therefore the production capacity of the winder.

2 Materials and Methods

The developed calculation model is based on open-source rotordynamic code ROSS [10]. ROSS is a python library based on beam Finite-element method that uses Timoshenko beam elements with gyroscopic effects. The code is based on the theory presented in [11]. The calculation routines already present in the program are adjusted for this research, as ROSS is unable to model interaction between multiple rotors or changing rotor geometries. This chapter presents the main concepts of the model creation procedure and how some of the unique features associated with two-drum winders are handled.

The created FE-model is used to run both modal analysis and forced response analyses. This means that the model assumes that the dynamics are not time-dependent, and steady state solution is sufficient. This was also assumed in [6]. Many of the key parameters in the two-drum winder change predictably during the winding cycle. The web speed does not depend on the winder state, and therefore can be given as a predefined function. The web speed is constant after initial acceleration, and the resulting rotational speeds are presented in Figure 2. Because the analysis is not time-dependent, there is no need to use simulation time as the dividing factor between the analysis steps. Instead, a more illustrative way is to divide the winding cycle into steps using different roll diameters. In the code created in this study, the model is updated for each paper roll diameter.

An example model is created with main parameters presented in Table 1, and it contains in total 8 rotors of which 4 are paper rolls. The model parameters are realistic considering real applications and selected based on values found in literature [6]. While for example the rotor properties can be effectively predicted, there is not much published knowledge available on the contact stiffness and damping in nips between paper rolls and steel rolls. This leaves a lot of parameters open for discussion.

2.1 Modeling principles

The two-drum winder can be represented as a system of rotors. In this case the system consists of four paper rolls on a shared axis, the 3 rotors used to support

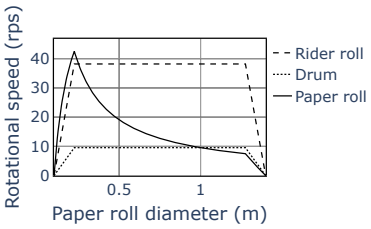

Fig. 2: Rotational speeds of different rolls during the winding cycle used in this investigation. As the paper roll diameter increases throughout the winding, its rotational speed is reduced to keep the web speed, i.e., surface speed, constant.

Table 1: Main parameters for the example winder model

Rotor	Outer diameter (m)	Inner diameter (m)
Steel Drum	1.00	0.95
Rider roll	0.25	0.20
Initial paper roll	0.10	0.05
Final paper roll	1.45	0.05

Rectangle beam	Width and height (m)	Wall thickness (m)
Rider roll beam	1.00	0.02

Parameter	Value	Unit
paper roll density	750	kg/m^3
Web speed	30	m/s
Number of rolls	4	-
Winder width	8	m
Element length	0.5	m

the paper rolls, and the rider roll beam supporting the rider roll as presented in Figure 1. For each rotor, a separate FE-model can be generated by ROSS, which includes the shaft elements and the bearing elements at the rotor end. Each node in the FE-models has 4 degrees of freedom (DOF), two lateral and two rotational. Axial and torsional DOFs are not included, as they are assumed insignificant to the problem at hand. The different rotor models are stored in the program, and are used later to create the different matrices needed in the FE-analysis of the whole winder.

The dynamics of the two-drum winder can be expressed with the following differential equation [11]

$$\mathbf{M}(d)\ddot{\mathbf{x}} + \mathbf{C}(d)\dot{\mathbf{x}} + \mathbf{G}(d)\boldsymbol{\Omega}(d)\dot{\mathbf{x}} + \mathbf{K}(d)\mathbf{x} = \mathbf{f}(d) \tag{1}$$

In this equation, $\mathbf{M}$ is the mass matrix and $\mathbf{K}$ the stiffness matrix, while $\mathbf{C}$ and $\mathbf{G}$ are the damping and gyroscopic matrices. $\mathbf{f}$ is the force vector and $\mathbf{x}$ is the nodal displacement vector. $\boldsymbol{\Omega}$ is the rotational speed matrix used to apply the correct rotational speed to the matching element. Most of the matrices change as function of the paper roll diameter d, and therefore need to be updated for each roll diameter. For the whole winder, the global system matrices $\mathbf{M}$, $\mathbf{K}$, $\mathbf{C}$ and $\mathbf{G}$ are assembled from individual roll matrices. The different rotor matrices are inserted in the global matrix diagonally so that the rotors do not share any

DOFs. The desired DOFs in the **K** and **C** matrices are coupled using spring and damper elements. The process is automated to create a connected rotor system.

It is important to note that the paper roll diameter is constantly changing during the winding cycle, meaning that the system is highly non-linear. The winding cycle can be divided into finite amount of steps representing a single paper roll diameter, during which the system can be assumed being linear. For each calculation case, all of the system matrices are updated with matching paper roll diameter.

2.2 Contact modelling

One of the key features in the winder simulation model is the nip contact between the paper roll and drums. In finite-element modelling with beam elements, this is usually addressed using springs and dampers that are inserted between contacting nodes. The springs represent the elastic part of the rolling contact, and the dampers are used to model the internal damping of the nip. The damping is due to local deformations and internal slippage between the paper layers inside the paper roll. The damping magnitude is highly dependent on the web material and the friction coefficient between layers [4]. The radial part of the contact can either be obtained from paper stack compression tests [12], or from 2D finite-element models [13, 14]. Contact mechanical study for the nip contact including the tangential contact has been conducted in [15]. The nip parameters used in this study are chosen based on values found in literature [6].

To model the nip contact between a single roll and drum, two spring and damper elements are used. The general arrangement for spring and damper elements for a single roll is presented in figure 3. The same pattern is repeated for each roll. While the nip contact is flexible in nature, this does not apply for all of the contacts in the model, such as connections between the rider roll and rider roll beam. To avoid introducing artificial compliance to the system, rigid couplings are used in these locations. A pinned coupling is selected for the connection between the paper rolls, as no better value has been proposed in the literature.

The nip contact has both radial and tangential components, and they do not necessarily have equal magnitude. Each contact component is represented with a spring and a damper element. The matrix form of a single spring element is the following:

$$\mathbf{K}_{\text{spring}} = \begin{bmatrix} k & -k \\ -k & k \end{bmatrix} \otimes \begin{bmatrix} \cos^2 \alpha(d) & \cos \alpha(d) \cdot \sin \alpha(d) \\ \cos \alpha(d) \cdot \sin \alpha(d) & \sin^2 \alpha(d) \end{bmatrix} \tag{2}$$

where k is the stiffness of the spring, α is the angle of the spring dependent on the paper roll diameter d and $\otimes$ is the Kronecker product. This results in a 4x4 matrix, which is then divided into 4 2x2 matrices, and inserted into the global matrix on the place of corresponding DOFs. For damper element, same procedure is applied. The spring angle α is defined so that the 0 degrees angle is along positive X-axis (Machine direction), and 90-degree angle in positive Y-axis (Vertical direction), as defined in Figure 1. The angle between paper rolls

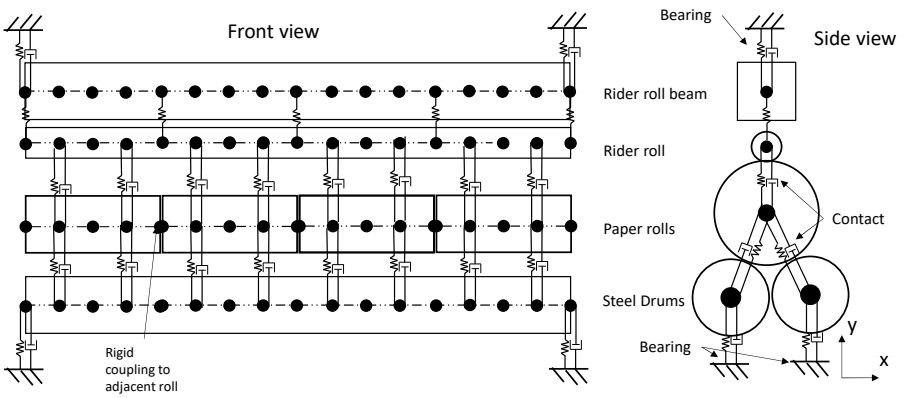

Fig. 3: Arrangement of springs and dampers connecting the different parts of the model. Only radial springs and dampers are shown in the figure, while tangential ones are hidden. Black dots represent nodes. There are four paper rolls adjacent to each other in the figure, and their lateral DOFs are coupled at the end nodes. There are no dampers between the rider roll and the rider roll beam.

and supporting drums needs to be updated during the analysis. The distance between two drums stays constant, but the distance between drum and roll axes increases and is equal to the sum of the two radiuses. This leads to the roll center position moving vertically as more material is wound onto the roll. For each calculated diameter, the spring matrices must be recalculated as part of the system matrix update routine.

2.3 Excitation due to roll unbalance

At the beginning of the winding cycle, the paper web is wound around cardboard cylinders, also called cores. In previous research [4], it has been observed that the roll core moves from rotational center towards the edge during the winding cycle. Additionally, the vibrations due to roll bouncing are measured at the same frequency as the roll rotational speed [16]. It is assumed that these two observations are connected, and the core eccentricity results in mass unbalance in the paper roll. The unbalance force magnitude due to roll eccentricity is assumed to equal [11]

$$f = e(d) \cdot m(d) \cdot \Omega(d)^2 \tag{3}$$

where e is the roll mass eccentricity, m is the roll mass per unit length and Ω is the rotational speed. In this model, all of the parameters depend on the paper roll diameter. The load of this magnitude is applied to all roll nodes. The load magnitude for each node includes mass equal to the length of one paper roll element. For simplicity, all loads act at the same phase. The mass eccentricity profile of the paper roll needs to be defined before the analysis, as there is no

feedback from system vibrations to paper roll unbalance. In this paper, 0.1% of roll diameter is used for the mass eccentricity value. The unbalance excitation is calculated for each roll diameter to match the changing rotational speed and roll mass.

3 Results

3.1 Modal analysis

By assembling the winder model according to principles presented in the previous section, the natural frequencies of the system can be solved for each roll diameter. The calculated values for the example system are presented in the upper part of Figure 4. Each line represents a natural frequency, and shows how they evolve as a the paper roll diameter increases. The modes for rider roll beam are colored in (a) and modes for front drum are colored in (b). The grey lines represent modes for other components, the paper rolls and rear drums. The plots includes all system natural frequencies below the maximum roll rotational speed, which is in this case equal to 45 Hz. Figure 4 shows that there are multiple natural frequencies in the operational speed range. In addition, most of the frequencies decrease as the paper roll diameter increases and mass is added to the winder. The natural frequency plots in Figure 4 show that it is impossible to avoid crossing the natural frequencies during winding cycle and therefore, resonance is inevitable. The figure also shows that some of the modes are not considerably effected during the cycle. These modes are associated to the front and rear drums.

Figure 5 shows two winder vibration mode shapes, one horizontal (a) and one vertical (b). In Figure 5(a), the modal displacement is mostly in horizontal direction, and in Figure 5(b) the displacements are in vertical direction. Most of the winder moves in unison, although in both modes the steel drums have much smaller displacement magnitudes due to their higher stiffness. The modes presented in 5 are not the only roll bouncing modes present, but they are the most significant contributors to the vibration response.

3.2 Forced response

A forced response for the winder system was calculated for each paper roll diameter. The load was predefined as described in chapter 2, and a steady-state solutions were calculated. The vibration velocity magnitudes for selected nodes are presented in the lower part of Figure 4. The nodes for which the results are displayed are located in the middle of rider roll beam and at the middle of front drum. Results for both machine direction (X-axis) and vertical direction are presented. Vertical dashed lines are shown when roll rotating frequency intersects with a system natural frequency.

The response in rider roll beam increases well before the load frequency intersects with the mode natural frequency. This is due to the high damping of roll to drum contact. As with any vibrating system, increasing damping not only

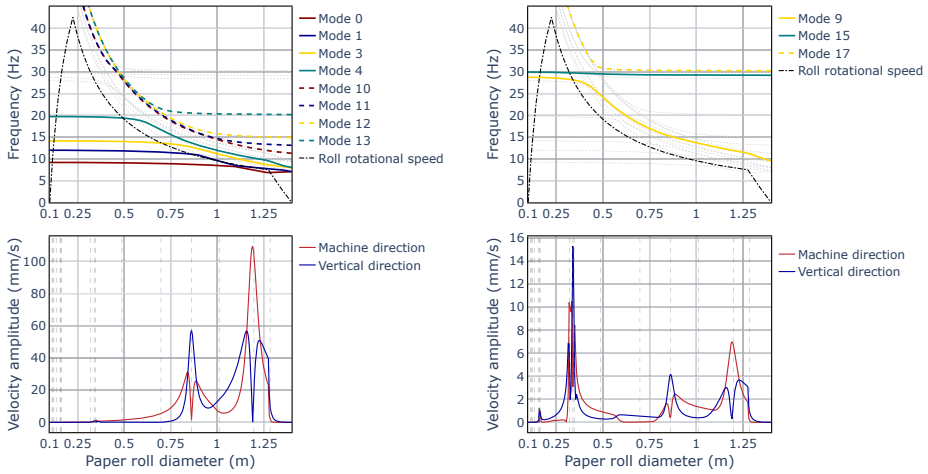

(a) Rider roll beam (b) Front drum

Fig. 4: Natural frequencies as a function of paper roll diameter (top) and maximum vibration velocity amplitudes (bottom) with different roll diameters for rider roll beam (a) and front drum (b). The responses are taken from the center nodes of each component. The gray lines in natural frequency plots show the natural frequencies of the other components for the model. In the response plots, vertical dashed lines correspond to paper roll rotational frequencies crossing with natural frequencies.

flattens the resonance peak but also widens it. The high damping value for the contact is supported by the observation that roll bouncing is more likely with webs that have a high internal friction coefficient [3]. This results in roll internal damping due to inter-layer slippage at the contact nip.

4 Discussion

The calculated results have good agreement with the previously observed results [3, 5]. In Figure 4 it was shown that the natural frequencies change considerably during the winding cycle due to accumulating roll mass in a similar fashion as in [5], including the similar veering phenomena. Additionally, the response amplitude results in Figure 4 pointed out that maximum response is obtained when the roll rotational speed intersects with the natural frequency of roll bouncing modes. In addition, especially the rider roll beam response starts to increase at roll diameters of 500 mm, which matches the observations in [16]. The roll bouncing modes shown in Figure 5 matched well with the bouncing description made in [3] from observing winder operation, as rolls move between the drums and at the same time excite the rider roll and its supporting beam. Previously published computational models have not been able to model this behavior in

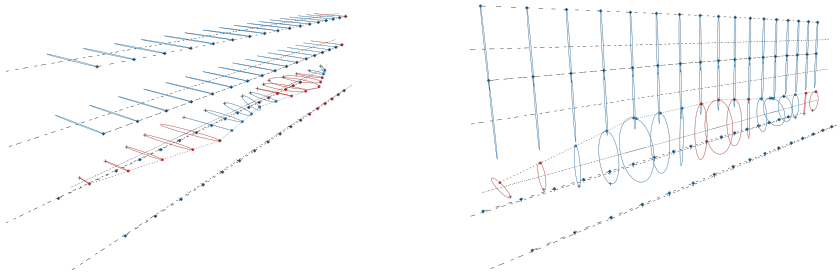

(a) Roll diameter 0.86m, ω_n=11Hz (b) Roll diameter 1.20m, ω_n=8Hz

Fig. 5: Two roll bouncing mode shapes with different roll diameters. Rider roll beam moves along the rolls. The natural frequency of the mode is given as ω_n. Each node is represented with dot, along with their vibration trajectories. Trajectory colors signify nodal whirl direction, blue means forward whirl and red means backwards whirl.

similar detail. The results indicate, that the model is able to capture roll bouncing phenomenon, while also providing further detail when compared to previous studies.

The observations made from the calculation results can be used to estimate the critical paper roll diameters for the winding cycle. It was also observed from Figure 4 , that some modes have no impact on the winder response. For example, at the paper roll diameter of 1000 mm, the roll rotational speed intersects a natural frequency, but no response increase is observed at the considered nodes. The mode in question has a backward whirl direction, which are not excited by loads rotating in the opposite direction [11]. In addition, the modes for different components are not independent of each other. Although the front drum modes are crossed quite early in the winding cycle, there are smaller response peaks when loading intersects with the rider roll beam modes. What stands out in the natural frequency plot in Figure 4 (b), is that by increasing the web speed, the roll rotational speed and the loading frequency is almost equal to the frequency of mode 9. This means that if the speed would be slightly increased, the winder would operate most of the winding cycle under resonance condition. This is undesired, and shows that the system stiffness must be increased in order to increase the production capacity.

5 Conclusions

Roll bouncing phenomenon was investigated. A rotordynamic model including the changing paper roll diameter and rotating speed, flexible rotors, gyroscopic effects and increasing unbalance load was developed. The computational analysis results show similar results as presented in previous research, including the changing natural frequencies and matching mode shapes. Based on modal and forced responses analyses, it is confirmed that the model is able to capture the roll

bouncing phenomenon adequately. The proposed model can more easily distinguish the difference between rigid body modes where rotors vibrate on bearings and rotor bending modes, which has not been present in previously published models. The critical parts of the winding cycle can also be estimated using the computational results. The model can be used to improve winder designs and to enhance winder production capabilities.

References

1. United Nations: Sustainable development goals, `https://www.un.org/sustainabledevelopment/`
2. Roisum, D.R., Walker, T.J., Jones, D.P.: The Web Handling Handbook. DEStech Publications, Incorporated (2021)
3. Olshansky, A.: Roll bouncing. Tappi journal 80(2), 99–107 (1997)
4. Roisum, D.R.: The mechanics of rollers. TAPPI (1996)
5. Jorkama, M.: The role of analytical winding dynamics in winder design. Tappi journal 81(1), 202–207 (1998)
6. Jorkama, M., Von Hertzen, R.: Wound roll generated unstable vibration on a two-drum winder. In: the Eight International Conference on Web Handling (IWEB). Oklahoma State University (June 2005)
7. Hou, X., Wang, Y., Feng, P., Yu, H., Ma, X., Chen, G.: A dynamic modeling approach for a high-speed winding system with twin-rotor coupling. Textile Research Journal 90(21-22), 2533–2551 (2020)
8. Kandadai, B., Good, J.: Winding virtual rolls. Tappi Journal 10(6), 25–31 (2011)
9. Mollamahmutoglu, C., Good, J., Markum, R., Gale, J.: Nip impinged center-winding including a nonlinear beam model. In: the Fourteenth International Conference on Web Handling (IWEB). Oklahoma State University (June 2017)
10. Timbó, R., Martins, R., Bachmann, G., Rangel, F., Mota, J., Valério, J., Ritto, T.: ROSS - Rotordynamic Open Source Software. The Journal of Open Source Software 5(48), 2120 (Apr 2020)
11. Friswell, M., Penny, J., Garvey, S., Lees, A.: Dynamics of Rotating Machines. Cambridge Aerospace Series, Cambridge University Press (2010)
12. Pfeiffer, J.D.: Measurement of the k2 factor for paper. Tappi journal (1981)
13. Ärölä, K., von Herzen, R.: Deformation of a Paper Roll Loaded Against a Nip Roller. In: Proceedings of the 18th Nordic Seminar On Computational Mechanics. pp. 55–58. Espoo, Finland (2005)
14. Mollamahmutoglu, C., Ganapathi, S., Good, J.K.: Pressures on webs in wound rolls due to winding and contact. Tappi journal 13, 41–50 (2014)
15. Jorkama, M.: Contact mechanical model for winding nip. Doctoral thesis, Helsinki University of Technology (2001)
16. Jorkama, M.: Winder vibration: Causes, defects, and remedies. In: the Eleventh International Conference on Web Handling (IWEB). Oklahoma State University (June 2011)